

# Synthesis Luminescent Plasmonic Silver Nanoparticles and The Chemical Affinity towards sulphur atom in Sulphide and Thiourea molecules: Ab-Initio DFT Study

Esam Bakir (✉ [ebakir@kfu.edu.sa](mailto:ebakir@kfu.edu.sa))

King Faisal University <https://orcid.org/0000-0003-3566-3579>

Ranjith Kumar Kamati

King Faisal University

---

## Research Article

**Keywords:** Luminescent Ag NPs, CTAB capping, Chemosensor, Sulphur molecules, Chemical affinity

**Posted Date:** October 21st, 2021

**DOI:** <https://doi.org/10.21203/rs.3.rs-792166/v1>

**License:** © ⓘ This work is licensed under a Creative Commons Attribution 4.0 International License.

[Read Full License](#)

---

---

# Synthesis Luminescent Plasmonic Silver Nanoparticles and The Chemical Affinity towards sulphur atom in Sulphide and Thiourea molecules: Ab-Initio DFT Study

Esam Mohamed Bakir<sup>1,2</sup> \* Ranjith Kumar Karnati<sup>1</sup>

Received: date / Accepted: date

## Abstract

Three different luminescent silver nanoparticles (AgNPs) were synthesized by simple reduction method with the different mole ratios of L-ascorbic/citrate solution and stabilized with CTAB. The prepared three AgNPs were characterized by UV, fluorescence, FTIR, dynamic light scattering measurements and Scanning Electron Microscopy. The plasmon bands of AgNPs-reddish-brown (RB), green (G) and reddish-green (RG) were centered at 565, 587 and 592 nm, respectively. The highly luminescence emission was observed for AgNPs(G). The size diameters of the prepared AgNPs-G, RG and (RB) were measured by dynamic light scattering (DLS) method at 24.3 nm, 66.28 nm and 103.46 nm, respectively. The electrochemical properties of AgNPs-RG was recorded the oxidative part of AgNPs into  $\text{Ag}^+$  at +0.23 V and the reduction part of  $\text{Ag}^+$  into  $\text{Ag}^0$  was recorded at -0.49 V vs.  $\text{Ag}/\text{AgCl}$ ). Cetyl trimethylammonium bromide (CTAB) was stabilized AgNPs(RG) which recorded in infrared and scanning electron microscope measurements. The concentration of thiourea, sodium sulphide was detected by the electrochemical sensitivity of AgNPs(RG)-CTAB. A calibration curve between electrochemical sensitivity of AgNPs-CTAB vs concentration of sulphur molecule. The limit of detection (LOD) was founded 2.10 and 1.90  $\mu\text{mole L}^{-1}$  of sodium sulphide and thiourea, respectively ( $R^2=0.94$ ,  $n=3$ ). The computational calculations are used to illustrated the chemical affinity of sulphur atom in sodium sulphide or thiourea towards AgNPs(RG).

---

\*Esam Mohamed Bakir

Department of Chemistry, College of Science, King Faisal University, AlAhsa 31982, Saudi Arabia

Department of Chemistry, Faculty of Science, Ain shams University, 11566, Cairo, Egypt

Correspondence author: E-mail: ebakir@kfu.edu.sa, <https://orcid.org/0000-0003-3566-3579>

Ranjith Kumar Karnati

Department of Chemistry, College of Science, King Faisal University, AlAhsa 31982, Saudi Arabia

E-mail: rkarnati@kfu.edu.sa

**Keywords:** Luminescent Ag NPs; CTAB capping; Chemosensor; Sulphur molecules; Chemical affinity.

## 1 Introduction

Silver nanoparticles AgNPs, have a unique properties like optical electronic properties and magnetic widely used in various fields such as catalytic and biological applications[1]. Silver nanoparticles (AgNPs) have prominent significance as analytical and bioanalytical sensors. The plasmonic fluorescence has significant importance due to widely used in a large number of scenarios ranging from biomedical research to optoelectronic devices. The fluorescence emission of plasmonic nanoparticles can be enhanced, quenched or spectrally shaped by controlling the near field interaction of sulphur molecules and silver nanoparticles. Generally, the fluorescence emission would be rapidly quenched when the sulphur molecules directly come into contact with plasmonic nano-silver due to the non-radiative energy transfer process[2] or dissociation of AgNPs into  $Ag^+$ . [3]The SPR phenomena of AgNPs is associated with the coupled oscillation of free electrons on the conduction band accompanying enhanced local electromagnetic field, which is intensely sensitive to surrounding medium conditions. When a nanoparticle is exposed to an electromagnetic wave, the electrons in the particle oscillate at the same frequency as the incident wave. silver nanoparticles exhibit various spectral characteristics, these are strongly dependent on their size, shape, interparticle spacing and environment[4]. The chemical reduction of silver salt into AgNPs using tris-sodium citrate as reducing agent was simple and famous method[5]. The shape and size diameter of AgNPs solution were dependent on pH values of medium. The size diameter of AgNPs was decreased by increasing pH value.[6]. Sui and et al studied the stability of AgNPs in the presence cetyl trimethylammonium bromide(CTAB) as a capping agent where CTAB molecules strongly bind to AgNPs with formation bilayer shell.[7]. Thiol and di-sulphide molecules can be quenched with change the redox cycle of AgNPs. Several research articles are interested to determinate the concentration of sulphur containing molecules such as thiourea, sodium sulphide and total sulphur contents in vegetables. Thiourea(TU) is common compound containing sulphur atoms and known as toxic and hazardous. It can lead to a disturbance of carbohydrate metabolism as well as chronic goitrogenic and other glandular problems in humans. Therefore, the determination of TU is of great importance.[8]. The silver nanoparticles sensor used in colorimetric method to detect thiourea (TU) amounts based on the changing of the absorption spectra of AgNPs plasmon band by adding different thiourea amounts[9]. The present method will introduce a simple and sensitive electrochemical method to determine the sulphur compounds based on the changes of redox peak of AgNPs(RG)-CTAB with addition of different amounts of sulphur molecules.

The present work will be introduced a simple reduction method for preparation of luminescent AgNPs with different mole ratio between citrate/L-ascorbic acid. The prepared AgNPs- reddish-brown (RB), green (G) and reddish-green (RG) are characterized with advanced UV-VIS, fluorescence, electroanalysis and dynamic light scattering (DLS) measurements, Scanning electron microscopy (SEM),. The factors affecting on the plasmon bands of the prepared AgNPs were studied by solvent polarity, pH values and the influences of cetyl trimethylammonium bromide(CTAB) as capping agent. The CTAB-stabilized AgNPs(RG) was used to determine the concentration of molecules containing sulphur atom such as sodium sulphide, thiourea (TU) and the total Sulphur present in vegetables. Density function theory (DFT) of optimized structure of thiourea and sodium sulphide was done. The computational calculations were used to expect the chemical affinity of sodium sulphide and thiourea to coordinate with AgNPs(RG). The analytical validation of the present method was applied.

## 2 Materials and Methods

Silver nitrate ( $AgNO_3$ ), trisodium citrate ( $Na_3C_6H_5O_7$ ), -L-ascorbic acid ( $C_6H_8O_6$ ), cetyl trimethylammonium bromide

(CTAB) sodium sulphide and thiourea were used in the experiment. All chemicals and solvents were received Sigma Aldrich (USA).

## 2.1 General Procedure for Synthesis of Silver Nanoparticles

The experimental technique, with slight modification to the existing method reported by Dads[10], has been applied for this study. In detail, 80 mL of 0.9 mmol L<sup>-1</sup> AgNO<sub>3</sub> and 20 ml mixture of 0.8 mmol L<sup>-1</sup> tris-sodium citrate and 1.0 mmol L<sup>-1</sup> ascorbic acid was heated with stirring till reach 60°C separately. Then added 20 ml of a solution to the 80 ml of AgNO<sub>3</sub> with vigorous stirring by maintaining 60°C for 20 minutes. After that, stopped heating, and the solution cooled to room temperature with continuous stirring. The color of colloidal solution was dependent on the molar ratio between ascorbic acid and citrate. The molar ratio between ascorbic / citrate was 10: 8, 8: 8, and 8:10 that gave AgNPs colors a reddish-green, Green and reddish-brown, respectively.

UV Shimadzu spectrophotometer and 4000-USBFL spectrofluorometer (Ocean Optics, Oceanview software, USA), was used to record the absorption and fluorescence spectra of AgNPs. Electrochemical analyses were performed using a Gamry 5000 potentiostat in a three-electrode system with a standard Ag/AgCl reference electrode (prepared in saturated KCl solution), Pt-wire as counter electrode, and gold working electrode (size diameter, 2 mm). The size diameter of AgNP colloidal solutions was measured by the dynamic light scatter (DLS) instrument model Nano DS, SN 161. The interaction and stabilization of AgNPs(RG)-CTAB was confirmed by the Fourier-transform infrared spectroscopy (FTIR) Alpha backer (OPUS software, USA) and Scanning electron microscopy (SEM) image of AgNPs(RG)-CTAB was obtained from Phillips CM201C microscope at 80 kV (Phillips, The Netherlands).

## 2.3 Computational Details

All DFT calculations of the chemical affinity of sodium sulphide and thiourea towards AgNPs were performed using the Gaussian G09W program. Geometry optimizations were conducted using density functional theory (DFT) with Beckers three parameter exchange functional [11], the Lee-Yang-Parr correlation functional (B3LYP) and the 6.31G(d) split-valence double zeta basis set was used [12]. After completing optimization, the theoretical properties of the studied compound such as Electron affinity (EA), Ionization energy (IE), hardness and softness and the HOMO, LUMO are recorded.

## 3. Results and Discussion

### 3.1 Characterization of AgNPs

The three different types of AgNPs were synthesized via slightly modified of Dads method by using citrate-ascorbic acid ratio [10]. The color of colloidal solutions of Ag NPs were observed as greenish(G), reddish green (RG) and reddish brown (RB). The absorbance spectra of the AgNPs-RB, AgNPs-G and AgNPs-RG shown a strong plasmon bands were centered at 565, 587 and 592 nm, respectively (see **Figure. 1(a)**). The bandwidth and band position of surface plasmon resonance (SPR) of AgNPs was dependent on the size diameter and the symmetrical shape of SPR band that indicates the AgNPs is spherical shape. [13, 14]. The surface plasmon band of AgNPs was affected by the changing of solvent polarity where the plasmon band was shifted to longer wavelength is called positive solvatochromism in polar solvents such as water, methanol and ethanol, while, the blue-shift was observed in less polar solvent (dimethylformamide) is called negative solvatochromism. The shift in peak position of AgNPs plasmon band was observed in polar solvents due to the agglomeration AgNPs with the change in the size diameter of AgNPs [15]. The origin of luminescence spectra of AgNPs(G), AgNPs (RG) and AgNPs(RB) were centered at 592, 587 and 565 nm, respectively. The strong luminescence intensity was observed of AgNPs(G) greater than AgNPs(RB) and AgNPs(RG) is attributed to the varied of energy gap (see **Figure. 1(b)**) [16] and fast recombination between e-LUMO

86 and hole-HOMO of AgNPs[17]. Approximation of Mie-Drude theory[18] can calculate the size diameter of the  
 87 AgNPs, The energy gaps of AgNPs(G), AgNPs(RB) and AgNPs(RB) were 2.48, 2.30 and 2.10 eV respectively,  
 88 according to Tauc relation plot[19].

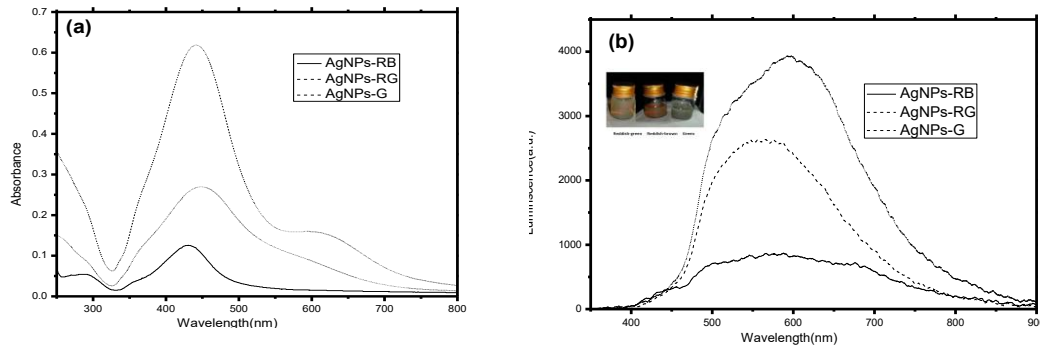


**Figure 1.** The UV-VIS (a) and luminescence spectra(b) of dispersed colloidal of AgNPs(RB), AgNPs (RG) and AgNPs(G) in ethanolic solution.

89 The Dynamic light scattering technique was used to measure the size diameter of the prepared AgNPs, especially in  
 90 the range of 2–500 nm[20]. The size diameters of AgNPs(G), AgNPs(RG) and AgNPs(RB) were recorded as 24.3 nm,  
 91 66.28 nm and 103.46 nm, respectively, Due to the influence of Brownian motion ,the size obtained from DLS is  
 92 usually larger than TEM[21]. The size and shape of AgNPs were dependent on the energy gap where the size of AgNPs  
 93 is inversible proportional to the size diameter[22]. The plasmon resonance shape of AgNPs was confirmed that AgNPs-  
 94 G, AgNPs-RG are monodispersed and AgNPs-RB is polydisperse due to the bright luminescence and weak  
 95 luminescence of AgNPs accordingly[23].

96 The electrochemical properties of AgNPs(RG) on the surface of electrode was recorded the oxidative part of AgNPs  
 97 into Ag<sup>+</sup> at +0.23 V and the reduction part of Ag<sup>+</sup> into Ag<sup>0</sup> was recorded at -0.49 V vs. Ag/AgCl) (see **Figure. 2**).  
 98 The voltammogram cycle of AgNPs was shown only one oxidative part in cycle of AgNPs is attributed to the high  
 99 size diameter of AgNPs[24].

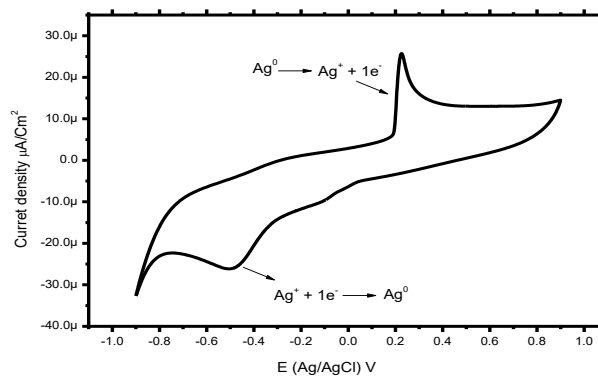


**Figure. 2.** shows typical cyclic voltammograms scan of the AgNPs(RG) evaluated in 10μM HCl as well as a bare glassy carbon electrode at scan rate 100mV/s.

105 The absorption spectra of AgNPs-RB at pH values in the range 02.50-10.00 was studied. The narrow and blue-shift of  
 106 the plasmon peak AgNPs-RB was recorded by raising the pH value where the changing of plasmon peak position of  
 107 AgNPs that indicates the size diameter was decreased, we conclude that raising the pH of the solution results in the  
 108 formation of nanoparticles with smaller size and vice versa. On the other hand, the broadening of the surface plasmon  
 109 resonance peak indicates the existence of a wider range of sizes in the solution [6].

### 111 3.2.The stabilization of the prepared AgNPs (RG)with CTAB

The absorption and luminescence spectra of AgNPs-RG are measured at different concentrations of CTAB in the range 0.1-0.9 mmol L<sup>-1</sup> (see **Figure 3(a)**). Without addition of [CTAB], the SPR band of citrate negative- AgNPs appeared at around 416 nm. The pre-micellar effect can be brought in fact that small aggregates of CTAB exist below the critical micellar concentration (CMC; 0.90 mmol L<sup>-1</sup>). The red shift of about 6 nm was observed by adding [CTAB] (from 0.1-0.9 mmol L<sup>-1</sup>), the shape of the AgNPs spectrum has been changed entirely (see **Figure 3(a)**). The decrease in the SPR band intensity with addition [CTAB] may be due to the sub, post and dilution-micellar effects. Finally, the CTAB interacts with AgNPs and protected from agglomeration effect [25]. The Photoluminescence of AgNPs was increased by adding more concentration of CTAB is attributed to the CTAB micelles interacted physically with the AgNPs and AgNPs incorporated into the micelles of CTAB and protect the AgNPs(RG)-luminescent form the quenching[7]. The electrochemical properties such as electroactivity of AgNPs(RG) was increased by adding initial concentration of CTAB due to the formation of small micelles of CTAB surrounded by AgNPs(RG) molecules. While in the higher concentration of CTAB, the inhibition of the electroactivity of AgNPs(RG) was observed due to the growth of CTAB large micelles around AgNPs(RG) and high frequency which leads to slowdown motion of AgNPs(RG) from bulk to surface of electrode(see **Figure 3(b)**)[26]

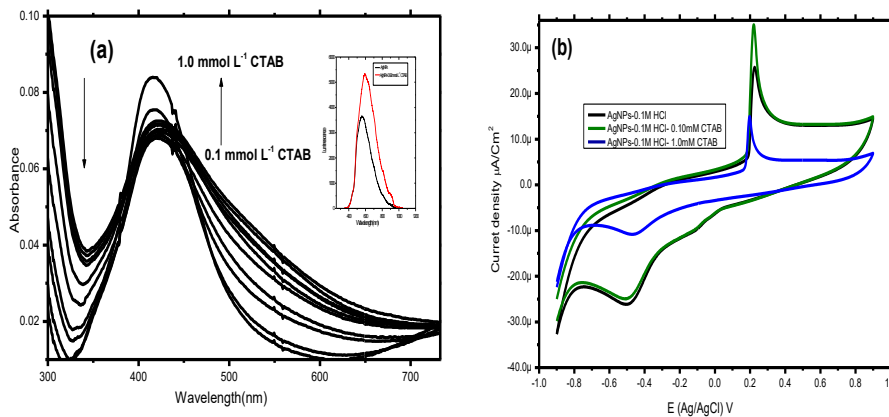


**Figure 3.** The absorption spectra (a) and the voltammograms scan(b) of the AgNPs-RG in 10 $\mu$ M HCl upon addition of CTAB at scan rate 100mV/s.

The interaction and stabilization between AgNPs(RG) with CTAB as capping agent was confirmed. The IR spectrum of CTAB possesses a strong and broad band at 3335.50 cm<sup>-1</sup> that can be attributed to the stretching vibrations of the ammonium group in CTAB. Peaks at 2923.93 cm<sup>-1</sup> and 2853.64 cm<sup>-1</sup> are attributed to two different C-H band vibrations of the -CH<sub>2</sub> group in CTAB. The band at 1635.71 cm<sup>-1</sup> followed by the band at 1472.94 cm<sup>-1</sup> corresponds to the asymmetric and symmetric stretching vibration of N<sup>+</sup>-CH<sub>3</sub>, respectively. [27] As for the CTAB-AgNPs, the broad absorption band at 3256.43 cm<sup>-1</sup> arose from the stretching vibration of the O-H bond of the water environment. The packing density in CTAB-capped Ag NPs is not so sufficient to produce any change in CH<sub>2</sub> stretching modes. The bandwidth change, however, reflects some changes from the structural order of the methylene chain groups in aggregate structure. Narrower bandwidths have been found to be resulted from a more ordered structure of the alkyl chains for bound CTAB molecules, which implies that CTAB molecules are arranged in some order on NPs surface.[28]

Scanning electron microscope images shown the AgNPs(RG) on the presence of CTAB in microscale diameter[29] The CTAB was stabilized the AgNPs via formation of micelles to protect it from agglomeration. The silver nanoparticles grown over the large particle size of CTAB (see Figure 4(b))

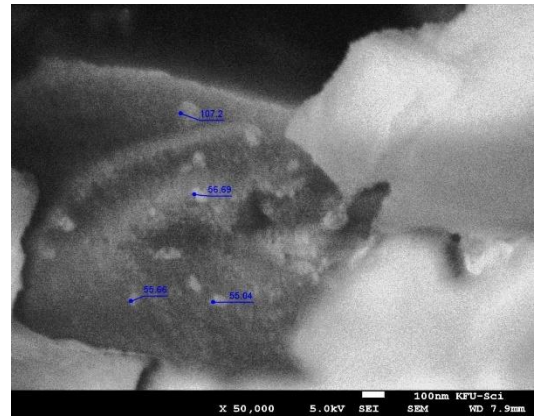
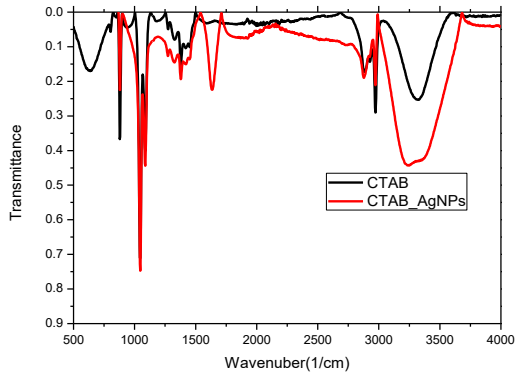


**Figure 4.** The IR spectrum (a) and SEM image(b) of AgNPs(RG)-CTAB system

142

143

### 3.3 The Chemical Affinity of AgNPs(RG)-CTAB Towards Sulphide and Thiourea

144

145

146

147

148

149

150

151

152

153

154

155

156

157

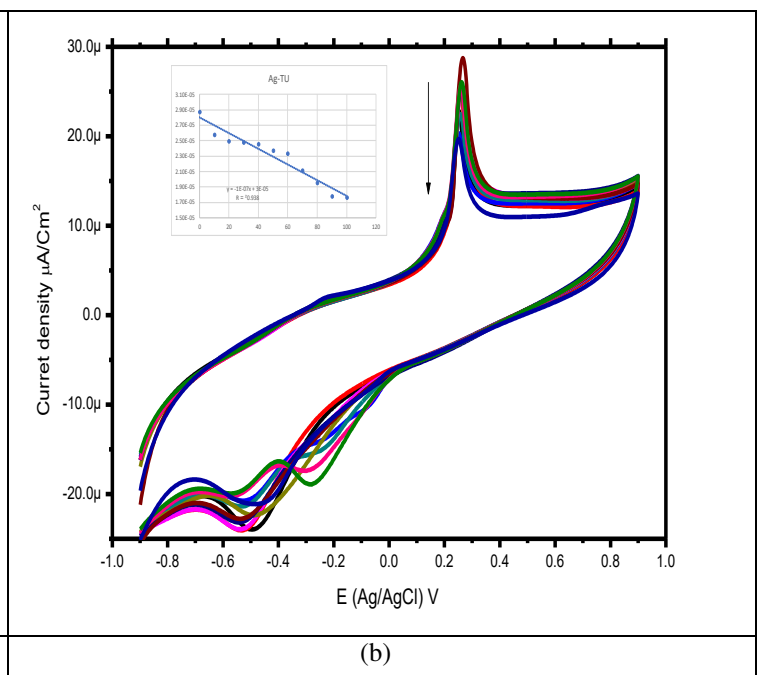
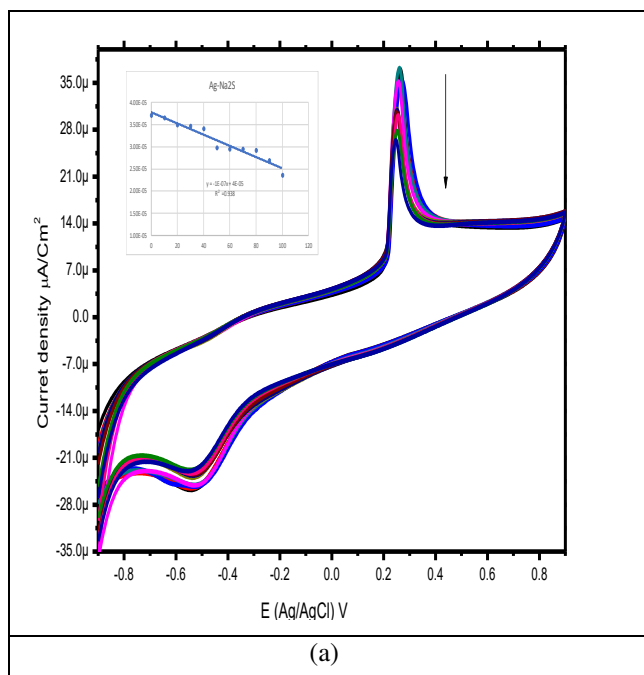


**Figure 5.** Represented the CVs scan of the AgNPs-RG/CTAB in 10 $\mu$ M HCl upon addition of 10-100  $\mu$ mol l<sup>-1</sup> of Na<sub>2</sub>S (a) and TU(b) (insert calibration curve at oxidation peak of AgNPs-RG/CTAB upon addition of 10-100  $\mu$ mol l<sup>-1</sup> of Na<sub>2</sub>S (a) and TU(b))

**Table 1.** The analytical validation parameters of sodium sulphide and thiourea.

Sulphur molecules ( $\mu$ g L <sup>-1</sup> ), n=3	*LOD	*LOQ	Correlation coefficient (R <sup>2</sup> )	R.S.D % <02.00%
Sodium sulphide	2.10	4.40	0.94	0.20
Thiourea	1.90	5.70	0.94	0.18

The Energy of the HOMO is directly related to the ionization potential and LUMO Energy is directly related to the electron affinity. Stability of the structures can be determined by the energy difference between HOMO and LUMO orbitals which is known as energy gap. The energy gap is used in determining molecular electrical transport properties. In addition, according to Koopmans' theorem the energy gap, E gap, defined as the difference between HOMO and LUMO energy(see equation (1)) [34].

$$E_g = (E_{HOMO} - E_{LUMO}) \cong IP - EA \quad (1)$$

The charge values are played important role to detect the chemical affinity of this sulphur molecules towards reaction with AgNPs. HOMO and LUMO energy values are useful to estimate Ionization potential (I) and Electron affinity (A) by the following **equation (1) and (2)**. The data of HOMO, LUMO gap, ionization potential, and electron affinity are given in **Table 2** and **equations (2) and (3)**.

$$IP = -E_{HOMO} \quad (2)$$

$$EA = -E_{LUMO} \quad (3)$$

The HOMO and LUMO energies are used for the determination of global reactivity descriptors. It is important that, hardness ( $\eta$ ) and softness (S) (see **equations (4) and (5)**) be put into a molecular orbital's framework[35]. We focus on the HOMO and LUMO energies in order to determine the interesting molecular/atomic properties and chemical quantities. These are calculated as following equations given in **Table 2**.

$$(\eta) = \frac{I-A}{2} \quad (4)$$

$$(S) = -\frac{1}{\eta} \quad (5)$$

**Table 2.** The chemical reactivity parameter such as electron affinity and softness of sulphide and thiourea.

Sulphur molecules	EHOMO (eV)	ELUMO (eV)	Eg (eV)	$\eta$ (Hardness)	S (softness)
Na <sub>2</sub> S	-4.5	-1.2	-3.3	3.91	0.26
TU1	-6.8	0.4	-7.2	7.04	0.14
TU2	-5.8	-1.7	-4.1	4.96	0.20

The higher values of softness(S) of sulphur molecules were observed in sodium sulphide. The reason is chemical affinity in sodium sulphide due to the formation of Ag<sub>2</sub>S-molecules[30]

## Conclusion

The chemical reduction method was used to prepare silver nanoparticles AgNPs, the ascorbic acid was used as a reducing agent and sodium citrate as a stabilizing agent. The ratio between ascorbic acid /sodium tris-citrate played important role to give three different colored AgNPs (reddish green, reddish brown and green). The absorbance spectra

of the AgNPs(RB), AgNPs(G) and AgNPs(RG) are shown a strong plasmon bands were centered at 565, 587 and 592 nm, respectively, this is the evidence for the formation of three different silver nanoparticles. The pH values were affected on the size diameter of the AgNPs by observing the shift of plasmon band, where the pH value increases, the surface plasmon peak shifts to left indicating a decrease in the size of the prepared nanoparticles. The CTAB was stabilized the AgNPs via formation of micelles to protect it from agglomeration. The plasmon behavior was shown the chemical affinity AgNPs(RG)-CTAB towards the small and bigger sulphur molecules. The highly softness(S) was observed in sulphide molecule to coordinate with AgNPs-CTAB. The sensitivity of AgNPs(RG)-CTAB chemosensor achieved in the present work for the determination of the total sulfur compounds in vegetables.

**Funding:** This work was supported by the Deanship for Scientific Research (DSR) at King Faisal University P.O box 400, Al-Ahsa, post code: 31982, Kingdom of Saudi Arabia, under Nasher Track (Grant No186360).

**Conflicts of interest:** "There are no conflicts to declare".

**Availability of data and material:** "All data is provided in full in the results section of this paper".

**Declarations:** Not applicable.

**Code availability:** Gaussian G09W program

**Author Contributions:** Conceptualization was done by all authors, Esam Mohamed Bakir and Ranjith Kumar Karnati; methodology, Esam Mohamed Bakir and Ranjith Kumar Karnati; software, Esam Mohamed Bakir; validation, Esam Mohamed Bakir; formal analysis, Esam Mohamed Bakir; investigation, Esam Mohamed Bakir.; resources, Esam Mohamed Bakir and Ranjith Kumar Karnati.; data curation, Esam Mohamed Bakir and Ranjith Kumar Karnati; writing—original draft preparation, Esam Mohamed Bakir, writing—review and editing, Esam Mohamed Bakir and Ranjith Kumar Karnati; visualization, Esam Mohamed Bakir; supervision, Esam Mohamed Bakir; project administration, Esam Mohamed Bakir and Ranjith Kumar Karnati; funding acquisition, Esam Mohamed Bakir.

## References

1. Jamila N, Khan N, Hwang IM, Saba M, Khan F, Amin F, Khan SN, Atlas A, Javed F, Minhaz A. (2020) Characterization of natural gums via elemental and chemometric analyses, synthesis of silver nanoparticles, and biological and catalytic applications. *Int J Biol Macromol.*147:853-866.
2. Badshah MA, Koh NY, Zia AW, Abbas N, Zahra Z, Saleem MW. (2020) Recent Developments in Plasmonic Nanostructures for Metal Enhanced Fluorescence-Based Biosensing. *Nanomaterials.*10(9):1749.
3. Liu J, Sonshine DA, Shervani S, Hurt RH. (2010) Controlled release of biologically active silver from nanosilver surfaces. *ACS Nano.*4(11):6903-6913.
4. Matsui M, Nakamura H. (2020) Plasmon resonance shift and near electric field of silver nanoparticles: Theoretical analysis of size, shape, and aggregation effects. *APS.*
5. Li P, Zou X, Wang X, Su M, Chen C, Sun X, Zhang H. (2020) A preliminary study of the interactions between microplastics and citrate-coated silver nanoparticles in aquatic environments. *J Hazard Mater.*385:121601.
6. Alqadi M, Noqtah OA, Alzoubi F, Aljarrah K. (2014) pH effect on the aggregation of silver nanoparticles synthesized by chemical reduction. *MATER SCI-POLAND.*32(1):107-111.
7. Sui Z, Chen X, Wang L, Xu L, Zhuang W, Chai Y, Yang C. (2006) Capping effect of CTAB on positively charged Ag nanoparticles. *Phys E: Low-Dimens Syst Nanostructures.*33(2):308-314.
8. Giri SN, Combs AB. (1970) Sulfur-containing compounds and tolerance in the prevention of certain metabolic effects of phenylthiourea. *oxicol Appl Pharmacol.*16(3):709-717.
9. Pedre I, Battaglini F, Delgado GJL, Sánchez-Loredo MG, González GA. (2015) Detection of thiourea from electrorefining baths using silver nanoparticles-based sensors. *Sens Actuators B Chem.*211:515-522.

- 238 10. Dadosh T. (2009) Synthesis of uniform silver nanoparticles with a controllable size. *Mater*  
239 *Lett.*63(26):2236-2238.
- 240 11. Becke AD. (1993) A new mixing of Hartree–Fock and local density-functional theories. *J Chem*  
241 *Phys.*98(2):1372-1377.
- 242 12. Koch W, Holthausen MC. (2015) A chemist's guide to density functional theory. John Wiley &  
243 Sons.
- 244 13. Amendola V, Bakr OM, Stellacci F. (2010) A study of the surface plasmon resonance of silver  
245 nanoparticles by the discrete dipole approximation method: effect of shape, size, structure, and  
246 assembly. *Plasmonics.*5(1):85-97.
- 247 14. Mehrdel B, Othman N, Aziz AA, Khaniabadi PM, Jameel MS, Dheyab MA, Amiri I. (2020)  
248 Identifying Metal Nanoparticle Size Effect on Sensing Common Human Plasma Protein by Counting  
249 the Sensitivity of Optical Absorption Spectra Damping. *Plasmonics.*15(1):123-133.
- 250 15. Prasad B, Arumugam SK, Bala T, Sastry M. (2005) Solvent-adaptable silver nanoparticles.  
251 *Langmuir.*21(3):822-826.
- 252 16. Poteau R, Heully J-L, Spiegelmann F. (1997) Structure, stability, and vibrational properties of  
253 small silver cluster. *Zeitschrift für Physik D Atoms, Molecules and Clusters.*40(1):479-482.
- 254 17. Duque J, Blandón J, Riascos H. (2017) Localized Plasmon resonance in metal nanoparticles using  
255 Mie theory. *Journal of Physics: Conference Series: IOP Publishing.* p. 012017.
- 256 18. Born M, Wolf E. (1980) Basic properties of the electromagnetic field. *Principles of optics.*44.
- 257 19. Tauc A. (1966) J., Grigorovici, R., vancu, "Tauc *J Phy. stat. sol.* 15, 627 (1966). pdf,". *Mater Res*  
258 *Bull.*3(1):37-46.
- 259 20. Tomaszewska E, Soliwoda K, Kadziola K, Tkacz-Szczesna B, Celichowski G, Cichomski M,  
260 Szmaja W, Grobelny J. (2013) Detection limits of DLS and UV-Vis spectroscopy in characterization  
261 of polydisperse nanoparticles colloids. *J Nanomater.*2013.
- 262 21. Igarashi E. (2015) *Nanomedicines and Nanoproducts: Applications, Disposition, and Toxicology*  
263 *in the Human Body.* CRC Press.
- 264 22. Singh M, Goyal M, Devlal K. (2018) Size and shape effects on the band gap of semiconductor  
265 compound nanomaterials. *J Taibah Univ Sci J TAIBAH UNIV SCI.*12(4):470-475.
- 266 23. Suslov A, Lama P, Dorsinville R. (2015) Fluorescence enhancement of Rhodamine B by  
267 monodispersed silver nanoparticles. *Opt Commun.*345:116-119.
- 268 24. Giovanni M, Pumera M. (2012) Size dependant electrochemical behavior of silver nanoparticles  
269 with sizes of 10, 20, 40, 80 and 107 nm. *Electroanalysis.*24(3):615-617.
- 270 25. Bae E-J, Park H-J, Park J-S, Yoon J-Y, Kim Y-H, Choi K-H, Yi J-H. (2011) Effect of chemical  
271 stabilizers in silver nanoparticle suspensions on nanotoxicity. *Bull Korean Chem Soc B KOREAN*  
272 *CHEM SOC.*32(2):613-619.
- 273 26. Toh H, Compton R. (2015) Electrochemical detection of single micelles through 'nano-impacts'.  
274 *Chem.*6(8):5053-5058.
- 275 27. Elfeky SA, Mahmoud SE, Youssef AF. (2017) Applications of CTAB modified magnetic  
276 nanoparticles for removal of chromium (VI) from contaminated water. *J Adv Res.*8(4):435-443.
- 277 28. Li H, Tripp CP. (2004) Use of infrared bands of the surfactant headgroup to identify mixed  
278 surfactant structures adsorbed on Titania. *J Phys Chem B.*108(47):18318-18326.
- 279 29. Jin W, Liang G, Zhong Y, Yuan Y, Jian Z, Wu Z, Zhang W. (2019) The Influence of CTAB-  
280 Capped Seeds and Their Aging Time on the Morphologies of Silver Nanoparticles. *Nanoscale Res*  
281 *Lett.*14(1):1-11.
- 282 30. Zhao L, Zhao L, Miao Y, Liu C, Zhang C. (2017) A colorimetric sensor for the highly selective  
283 detection of sulfide and 1, 4-dithiothreitol based on the in situ formation of silver nanoparticles using  
284 dopamine. *Sens.*17(3):626.
- 285 31. Zhang J, Malicka J, Gryczynski I, Lakowicz JR. (2004) Oligonucleotide-displaced organic  
286 monolayer-protected silver nanoparticles and enhanced luminescence of their salted aggregates. *Anal*  
287 *Biochem.*330(1):81-86.

- 288 32. Dave S. (2018) Electrochemical and spectral characterization of silver nanoparticles synthesized  
289 employing root extract of *Curculigo orchioides*. *Indian J Chem Technol.*25(2):201-207.
- 290 33. Wang G-L, Dong Y-M, Zhu X-Y, Zhang W-J, Wang C, Jiao H-J. (2011) Ultrasensitive and  
291 selective colorimetric detection of thiourea using silver nanoprobos. *ANLST.*136(24):5256-5260.
- 292 34. Bredas J-L. (2014) Mind the gap! *Mater Horiz.*1(1):17-19.
- 293 35. Fukui K, Yonezawa T, Shingu H. (1952) A molecular orbital theory of reactivity in aromatic  
294 hydrocarbons. *J Chem Phys.*20(4):722-725.
- 295